Published in final edited form as:
Virus Res. 2010 January ; 147(1): 17–24. doi:10.1016/j.virusres.2009.09.013.

Moussa virus: a new member of the *Rhabdoviridae* family isolated from *Culex decens* mosquitoes in Côte d'Ivoire

Phenix-Lan Quan[1,†], **Sandra Junglen**[2,†,*], **Alla Tashmukhamedova**[1], **Sean Conlan**[1], **Stephen K. Hutchison**[3], **Andreas Kurth**[4], **Heinz Ellerbrok**[4], **Michael Egholm**[3], **Thomas Briese**[1,*], **Fabian H. Leendertz**[2], and **W Ian Lipkin**[1]

[1]Center for Infection and Immunity, Mailman School of Public Health, Columbia University, New York, NY, USA

[2]Research Group Emerging Zoonoses, Robert Koch-Institut, Berlin, Germany

[3]454 Life Sciences, Branford, CT, USA

[4]Center for Biological Safety, Robert Koch-Institut, Berlin, Germany

Abstract

Characterization of arboviruses at the interface of pristine habitats and anthropogenic landscapes is crucial to comprehensive emergent disease surveillance and forecasting efforts. In context of surveillance campaign in and around a West African rainforest, particles morphologically consistent with rhabdoviruses were identified in cell cultures infected with homogenates of trapped mosquitoes. RNA recovered from these cultures was used to derive the first complete genome sequence of a rhabdovirus isolated from *Culex decens* mosquitoes in Côte d'Ivoire, tentatively named Moussa virus (MOUV). MOUV shows the classical genome organization of rhabdoviruses, with five open reading frames (ORF) in a linear order. However, sequences show only limited conservation (12–33% identity at amino acid level), and ORF2 and ORF3 have no significant similarity to sequences deposited in GenBank. Phylogenetic analysis indicates a potential new species with distant relationship to Tupaia and Tibrogargan virus.

Keywords

Moussa rhabdovirus; Culex decens mosquitoes; Phylogeny; High-throughput pyrosequencing; Ivory Coast; Africa

1. Introduction

The family *Rhabdoviridae* includes six genera whose members infect a wide range of animals and plants (Tordo et al., 2005). Viruses in the genus *Lyssavirus*, such as rabies virus, infect

*Corresponding author. Mailing address for T. Briese: Center for Infection and Immunity, Mailman School of Public Health, Columbia University, 722 West 168th Street, New York, NY 10032, USA; Phone: 212-342-9031; Fax: 212-342-9044; thomas.briese@columbia.edu. Mailing address for S. Junglen: Research Group Emerging Zoonoses, Robert Koch-Institute, Nordufer 20, D-13353 Berlin, Germany; Phone: +49 30 45472592; Fax: +49 30 45472181; JunglenS@rki.de.
†both authors contributed equally to this work

humans and other mammals, frequently causing fatal encephalopathy (Lyles and Rupprecht, 2007). Major vertebrate pathogens are found in the genera *Vesiculovirus* and *Ephemerovirus* (livestock), and *Novirhabdovirus* (fish). The *Cytorhabdovirus* and *Nucleorhabdovirus* genera include plant pathogens. The *Rhadoviridae* also include six unassigned serogroups as well as non-classified species (Bourhy et al., 2005; Tordo et al., 2005).

Rhabdoviruses have negative, single-stranded RNA genomes encoding at least five proteins: a nucleoprotein (N), phosphoprotein (P), matrix protein (M), glycoprotein (G) and a large RNA-dependent RNA polymerase (L). Genomes of viruses in the *Ephemerovirus*, *Novirhabdovirus*, *Cytorhabdovirus* and *Nucleorhabdovirus* genera include some additional short genes (Lyles and Rupprecht, 2007).

Arthropods play an essential role in the transmission of many rhabdoviruses (Tesh et al., 1972). Numerous plant-infecting rhabdoviruses are transmitted by leafhoppers, aphids or lacebugs (Nault, 1997). Arthropods can also transmit animal and human rhabdoviruses; mosquitoes transmit bovine ephemeral fever virus, and sandflies can transmit Chandipura virus (Dhanda et al., 1970; Tordo et al., 2005). Thus, identification of rhabdoviruses that disperse through arthropod vectors and may emerge as vertebrate pathogens (Aitken et al., 1984; Shope, 1982), is vital to comprehensive virus surveillance, and provides the foundation for improved disease prediction and forecasting efforts.

In the course of a surveillance campaign to assess the distribution of arboviruses and their vectors in rainforest edge habitats in West Africa, bullet-shaped particles were detected by electron microscopy in cell culture supernatants of cells infected with homogenates of trapped mosquitoes (Junglen et al. *EcoHealth* submitted). Although particle-associated nucleic acid PCR (Stang et al., 2005) allowed identification of small L sequence fragments consistent with the presence of a rhabdovirus, its genome structure and phylogeny remained elusive. Unbiased high-throughput pyrosequencing (UHTS), in combination with specific amplification using primers designed from the UHTS data enabled determination of the complete genome sequence. Sequence and phylogenetic analyses indicated a new member of the family *Rhabdoviridae*, tentatively named Moussa virus (MOUV), after the coffee plantation from which the first isolate (D24) originated.

2. Materials and Methods

2.1. Mosquito collection and virus culture

Mosquitoes were collected from February to June 2004 in different habitats in rainforest edge regions of Taï National Park, Côte d'Ivoire. Mosquitoes trapped in primary forest, secondary forest, coffee plantations, two villages and at a camp site in the primary forest were used for cell culture infection (Junglen et al., 2009). Filtered homogenates of female mosquitoes were used to inoculate *Aedes albopictus* C6/36 cell cultures (Igarashi, 1978) and 200 μL supernatant was passaged onto fresh cells when 70–90% of cells showed cytopathic effect (CPE). After 3 passages, viral stocks were generated, stored at −70°C, and used for further analyses.

Infectious C6/36 culture supernatant was applied to African green monkey (Vero), baby hamster kidney (BHK), porcine stable equine kidney (PSEK), 293, A549, and Hep2 cell lines, as well as to primary chicken embryo fibroblasts (PCF) at 1/10 and 1/100 dilutions. Every seven days 200 μL supernatant was transferred to fresh cells for a period of 21 days and cells were observed for an additional 8 days for signs of CPE. Culture supernatants were used for PCR and re-infection of C6/36 cell.

2.2. Virus purification

Culture supernatant of one T175 flask was harvested except for 5 mL that were left behind to cover cells for one cycle of freeze-thaw. Virus from the total clarified supernatant was pelleted through 5 mL of 36% sucrose (28,000 rpm, 4 h, 4°C, SW32 rotor; Beckman, Fullerton, CA, USA). Virus pellet was suspended overnight at 4°C in 140 μL phosphate buffered saline (PBS).

2.3. Electron microscopy

Aliquots of purified virus (10 μL) were fixed with 2% paraformaldehyde and processed for direct negative staining electron microscopy (Biel and Gelderblom, 1999; Hayat et al., 2000). 400-mesh copper grids covered with pioloform F and carbon were floated on sample drops, washed twice on drops of double-distilled water and contrasted with 1% uranyl acetate (60 mM, pH 4). Prepared grids were then examined by transmission electron microscopy with an FEI Tecnai G2 (FEI, Hillsboro, OR,USA).

2.4. RNA extraction, cDNA synthesis, and polymerase chain reaction (PCR)

Either 140 μL culture supernatant or 140 μL purified virus were subjected to RNA extraction with a Viral RNA Kit (Qiagen, Hilden, Germany). cDNA was generated using 0.5 μg total RNA, 10 pmol random hexamers and a Superscript cDNA synthesis Kit (Invitrogen, Carlsbad, CA, USA). PCR reactions to characterize multiple isolates were performed in 25 μL reactions containing 2 μL cDNA, 7.5 pmol of each primer (FWD-10143 and REV-10788; Table S1), and 1 unit Platinum Taq polymerase (Invitrogen). Cycle conditions were 1× 95°C/10 min, 35× 95°C/30 sec, 54°C/30 sec, 72°C/5 min, and 1× 72°C/10 min. PCR products were size-fractionated by electrophoresis in agarose gels, extracted with ExoSAP-IT® (USB, Cleveland, OH, USA), and then directly sequenced with ABI PRISM Big Dye Terminator Cycle Sequencing kits on ABI PRISM DNA Analyzers (Applied Biosystems, Foster City, CA, USA).

2.5. Unbiased High-Throughput Sequencing (UHTS)

Purified RNA (0.5 μg) was DNase I-digested (DNA-free; Ambion, Austin, TX, USA) and reverse transcribed using a Superscript II kit (Invitrogen) with random octamer primers linked to an arbitrary, defined 17-mer primer sequence (MWG, Huntsville, AL, USA). cDNA was RNase H-treated prior to random amplification by PCR, applying a 9:1 mixture of a primer corresponding to the defined 17-mer sequence, and the octamer-linked 17-mer sequence primer, respectively (Palacios et al., 2007). Products >70 bp were purified (MinElute, Qiagen) and ligated to linkers for sequencing on a GSL FLX Sequencer (454 Life Sciences, Branford, CT, USA)(Margulies et al., 2005). After trimming primer sequences and eliminating highly repetitive elements, sequences were clustered and assembled into contiguous fragments (contigs) for comparison by the Basic Local Alignment Search Tool (blast; (Altschul et al., 1990)) to the GenBank database at nucleotide (nt) and translated amino acid (aa) level applying blastn and blastx software (Cox-Foster et al., 2007; Palacios et al., 2008). The resulting alignments were further processed using custom software applications written in Perl (BioPerl 5.8.5) and programs accessible through the GreenePortal website (http://156.145.84.111/Tools).

2.6. Genome sequencing

PCR primers for amplification across sequence gaps were designed based on the UHTS data and the draft genome was re-sequenced by overlapping PCR products that covered the entire genome except for terminal sequences (Table S1). RNA was transcribed with Superscript II (Invitrogen; 20 μL assay volume) using random hexamers. PCR primers were applied at 0.2 μM concentration with 1 μL cDNA and HotStar polymerase (Qiagen). Products were purified (QIAquick PCR purification kit; Qiagen) and directly dideoxy-sequenced on both strands.

2.7. Rapid amplification of cDNA ends (RACE)

Genomic termini were characterized with 5'- and 3'-RACE kits (Invitrogen). Virus-specific primers for isolate D24 were: 5'-CCC CAG TTG GTA AGG GAA AT, located 913 nt from the 3'-genomic terminus for reverse transcription, 5'-GCC TTG TCC CTG AGG AAA CT, located 703 nt from the 3'-genomic terminus for first PCR with primer UAP (Invitrogen), and 5'-GTT CGT GCC GTT TTC GTA CT, located 528 nt from the 3'-genomic terminus for second PCR with primer AUAP (Invitrogen). RNA for the second RACE was tailed with poly (A) polymerase (Ambion) and purified using MEGAclear (Ambion). cDNA synthesis was primed with oligo d(T)-adapter primer AP (Invitrogen), and first PCR used primer 5'-TAG TCC ACA GCC TGG CTC AT, located 996 nt from the 3'-antigenomic terminus and primer UAP (Invitrogen), the second PCR used primer 5'-AAC TAC GGG TCC CCT TCA CT, located 738 nt from the 3'-antigenomic terminus and primer AUAP (Invitrogen). All primers were at 0.2 μM final concentration. PCR products were purified with QIAquick PCR purification kits (Qiagen) and directly dideoxy-sequenced in both directions.

2.8. Phylogenetic analysis

Deduced full-length and partial L aa sequence of MOUV was aligned with L-sequences of selected members of the family *Rhabdoviridae* and other *Mononegavirales* (see Table S2) using ClustalW (Thompson et al., 2002). Phylogenetic analyses were performed with programs from the MEGA package (http://www.megasoftware.net), applying a neighbor-joining model. Statistical significance was assessed by bootstrap re-sampling of 1000 pseudoreplicate data sets. Pairwise sequence similarity and identity were calculated using the Smith-Waterman algorithm implemented in the European Molecular Biology Open Source Software suite (EMBOSS)(Rice et al., 2000).

3. Results

3.1. Complete MOUV genome sequence

Complete MOUV genome sequence was determined using C6/36 cell culture supernatant from two isolates, C23 and D24, which showed characteristic morphology of a rhabdovirus (Fig. 1A). UHTS yielded approximately 90,000 sequence reads with a mean length of 170 nt. Nine contigs (858 sequence reads, mean length 227 nt), ranging in size from 142 nt to 2,681 nt were assembled that showed homology to L, G and N sequence of rhabdoviruses when aligned to the GenBank database (http://www.ncbi.nlm.nih.gov/Genbank) by blastn and blastx (Table 1, Fig. 1B); except for contig C, all other contigs were identified only by blastx search. The UHTS reads covered 8.8 kilobases (kb), representing 76.3% of a prototypic rhabdoviral genome. PCR amplification using specific primers designed on the UHTS data confirmed the presence of two isolates of MOUV, C23 and D24 (GenBank accession numbers FJ985748 and FJ985749). The 3'- and 5'-termini of the MOUV genome were characterized by RACE. Twenty clones for each isolate were sequenced. Both draft sequences were re-sequenced by overlapping PCR across the whole genome, indicating 96% sequence identity between both isolates at nt level.

The MOUV genome comprises 11,526 nt with a genomic organization characteristic for known members of the genera *Lyssavirus* and *Vesiculovirus* (Fig. 1B), including three open reading frames (ORF) with homology to rhabdoviral N, G and L proteins; two ORFs, located in the position of P and M genes in other rhabdoviruses showed no nt or aa homology in blast search to sequences deposited in GenBank. After completion of MOUV sequencing by PCR, retrospective analysis of the UHTS results revealed that a total of 1,572 reads matched the final sequence, covering 93.5 % of the genome including 31 sequence reads in ORF-2 and 352 sequence reads in ORF-3 (Table 2).

3.2. Open reading frames

ORF-1, nucleoprotein (N)—The N protein of rhabdoviruses binds genomic RNA to form an RNase-resistant ribonucleocapsid that serves as template for both transcription and replication by the large viral RNA-dependent RNA polymerase (Thomas et al., 1985). ORF-1 is predicted to code for an N of 468 aa (51 kDa). Pairwise comparison of deduced protein sequence indicated highest homology to N of vesicular stomatitis Indiana virus (VSIV; 23.5%) and Tupaia rhabdovirus (TUPV; 23%)(Table 3). Pairwise alignment of MOUV N with that of VSV and rabies virus also aligned residues identified as interacting with RNA (Albertini et al., 2006; Green et al., 2006; Luo et al., 2007) (data not shown); the highly conserved motif SPYS (Kouznetzoff et al., 1998) was present as S_{292}PYT in MOUV (Fig. S1). The alignment also indicates conserved aa clusters identified in rhabdoviruses infecting both, insects and vertebrates (dimarhabdoviruses; Kuzmin et al., 2006).

ORF-2, putative phosphoprotein (P)—ORF-2 of MOUV is composed of 870 nt that encode a polypeptide of 290 aa (32 kDa). The sequence is not similar to others in GenBank by blastn or blastx, or by hidden markov model alignments to the Pfam database (http://pfam.janelia.org). ORF-2 is located in the genomic position of P, which is an essential cofactor of the active viral transcriptase/replicase complex. Compared to P of other rhabdoviruses, ORF-2 shows highest aa identities to those of Wongabel virus (WONV; 20.9 %) and Flanders virus (FLAV; 19.6%)(Table 3). ORF-2 also comprises potential phosphorylation sites, including one tyrosine phosphorylation site and 30 serine/threonine phosphorylation sites. However, MOUV P lacks a casein kinase II motif found in domain I of VSV P (Barik and Banerjee, 1992;Chattopadhyay and Banerjee, 1987). A small ORF overlapping that of P may code for a putative C protein of 56 residues with a predicted pI of 12. Analysis of MOUV P using PROSITE, a database of functional protein domains and sites (http://ca.expasy.org/prosite), identified a C-terminal zinc finger C2H2-domain (C_{251}EKYGCQEPVTPSNWLHHHRSCH). To date, no zinc finger domain has been reported for a rhabdoviral P.

ORF-3, putative matrix protein (M)—ORF-3 is composed of 726 nt, encoding a 242 aa polypeptide (27 kDa). ORF-3 does not have apparent similarity or motifs common to other sequences. No functional domains were identified using PROSITE. ORF-3 is located in the genomic position of M, a gene that in other rhabdoviruses encodes a protein critical to virus morphology, assembly and budding (Desforges et al., 2001; Kopecky et al., 2001; Schmitt and Lamb, 2004). The highest aa identity was found with M of WONV (20.7 %) and FLAV (19%) (Table 3). It has been previously shown that M of rhabdoviruses can be phosphorylated (Kaptur et al., 1992; Tuffereau et al., 1985); ORF-3 of MOUV includes 14 serine, 4 threonine, and 2 tyrosine potential phosphorylation sites. Late domain motifs PPxY, P(T/S)AP, and YxxL (Chen and Lamb, 2008; Demirov and Freed, 2004) identified in the M proteins of rabies virus and VSV (Harty et al., 1999; Irie et al., 2004) and implicated in viral budding, are not present in MOUV M.

ORF-4, glycoprotein (G)—The G of rhabdoviruses mediates attachment to, and fusion with, the cell membrane during entry, and particle budding during exit. G is predicted to be coded by the 1,581 nt ORF-4 of MOUV, yielding a protein of 527 aa (60 kDa). Pairwise alignments with corresponding proteins of other rhabdoviruses indicated highest aa identity with G of infectious hematopoietic necrosis virus (IHNV; 23.2%) and VSIV (22.9%)(Table 3). Despite limited primary sequence conservation amongst G proteins of rhabdoviruses, general structural features including glycosylation sites, antigenic domains, and cysteines residues are commonly conserved (Coll, 1995;Walker and Kongsuwan, 1999). Accordingly, the G of MOUV shows features of type I glycoproteins, including an N-terminal 18 aa signal peptide predicted by SignalP (http://www.cbs.dtu.dk/services/SignalP), a COOH-terminal hydrophobic anchor

located at aa 463–485 and followed by a short cytoplasmic tail (aa 486–526), six potential glycosylation sites, and fourteen cysteine residues of which twelve comprise the conserved cysteines found in animal rhabdoviruses (C_I to C_{XII}; (Walker and Kongsuwan, 1999)).

ORF-5, large polymerase (L)—L is a component of the active ribonucleoprotein and necessary for transcription and replication. The L of MOUV is predicted to derive from the 2,142 aa ORF-5 (245 kDa). Comparison of deduced aa sequence of ORF-5 with L of other rhabdoviruses indicated highest identity with that of VSIV (32.6%) and TUPV (31.4%)(Table 3). RNA-dependent RNA polymerases (RdRp) of non-segmented negative-strand RNA viruses contain conserved residues clustered in six blocks designated I to VI (Poch et al., 1990). The four highly conserved motifs A through D (Poch et al., 1990;Poch et al., 1989) in block III are also conserved in L of MOUV (Table 4). In addition, conserved aa in block V, including the motif GxxT[n]HR involved in capping activity (Li et al., 2008), are present in MOUV L (G_{1166}xxT[69]HR_{1240}). Conserved aa in block VI shown to be involved in *S*-adenosyl-L-methionine interaction and cap methylation (Bujnicki and Rychlewski, 2002;Li et al., 2006) are also present in MOUV L (G_{1700}xGxGG[60]D_{1766}).

3.3. Gene junctions

Gene junctions in rhabdoviruses are composed of the polyadenylation signal for the upstream gene, a short intergenic region and the transcription initiation sequence for the downstream gene. In MOUV a putative polyadenylation signal was identified as 3’-GAACUUUUUUU, separated by 2–3 nt from a putative transcription initiation sequence 3’-UUGU(U/G)UG(G/C/A)U (Fig. 2A). The 5’-nontranslated regions of mRNA transcripts are 22 to 60 nt long, while the 3’-nontranslated regions are 10 to 83 nt long (Fig. 2A).

A common feature of rhabdovirus genomes is complementary of the 3’- and 5’-termini of the genome (Whelan et al., 2004). The 3’-leader and the 5’-trailer sequences of MOUV comprise 53 nt and 56 nt, respectively; with seventeen of the twenty-one terminal nt being complementary (Fig. 2B). The MOUV leader sequence contains the first three, and the tenth nt that are conserved in rhabdoviruses known to infect mammals (Fig. 2C).

3.4. Phylogenetic analyses

Phylogenetic analysis of short sequences can be misleading. Thus, we evaluated the complete 2,142 aa L ORF in comparison to available complete L sequences of other rhabdoviruses. The derived phylogenetic tree, which also includes selected members of other families of the order *Mononegavirales*, shows TUPV, isolated from tree shrews, as the closest match to MOUV (Fig. 3A). However, complete L sequence is only available for a limited number of rhabdoviruses. Thus, we also examined a partial L sequence dataset comprising 158 aa that represents not only the six recognized genera but also four additional monophyletic groups (Bourhy et al., 2005). Phylogenetic analysis in comparison to these sequences puts MOUV in a close relationship to the Australian Tibrogargan virus (TIBV)(Fig. 3B).

3.5. Multiple strains of MOUV

In addition to isolates C23 (from *Culex decens* mosquitoes of the secondary forest and D24 (from *Culex* mosquitoes of the adjacent Moussa coffee plantations), MOUV was also identified in five other of the 97 CPE-positive supernatants obtained from 437 pools tested (4,839 mosquitoes). These included two additional isolates from the secondary forest, two from the primary rainforest, and one from a camp in the primary rainforest (Table 5). All isolates induced comparable CPE with syncytia formation in C6/36 cells 3 to 22 days after inoculation. Sequence comparison of a 600 bp L gene amplification product generated from these isolates indicated a higher degree of conservation within isolates from the forest (98.6 – 100%), or the camp and the plantation (98.6%), than between those two groups (94.8 – 96.4%). Although

the isolates replicated stably in C6/36 cells, inoculation of vertebrate cell lines did not indicate signs of CPE (Vero, BHK, PSEK, 293, A549, Hep2, and PCF), or virus replication as assessed by PCR (PSEK).

4. Discussion

The 11,526 nt genome of MOUV comprises at least five ORFs. Three ORFs correspond to the N, G and L proteins characteristic of rhabdoviruses; two correspond in genome position to P and M, but are so dissimilar to known rhabdovirus sequences that we failed to appreciate their presence during the initial analysis. To our knowledge this is the first description of a complete genome sequence for a rhabdovirus isolated from mosquitoes.

Phylogenetic analyses performed with complete and partial L polymerase sequence indicates that although MOUV is related to the dimarhabdovirus supergroup (Bourhy et al., 2005), MOUV appears to be distinct from recognized genera and species. Complete L polymerase sequence suggests a relationship to TUPV, an as yet unclassified rhabdovirus identified in tree shrews tentatively assigned to the vesiculovirus genus (Springfeld et al., 2005; Tordo et al., 2005); however, analysis of a more comprehensive set of partial L polymerase sequences suggests a closer relationship to TIBV. TIBV, the sole member of the Tibrogargan group, was initially isolated in Australia from biting midges and cattle (Bourhy et al., 2005). Further genomic characterization of the TIBV genome may provide insights into the phylogenetic relationship between these viruses. The only rhabdovirus previously known to originate from Côte d'Ivoire is Nkolbisson virus (NKOV), a member of the Kern Canyon group that was isolated from *Aedes* mosquitoes and characterized based on serology and electron microscopy (http://www.pasteur.fr/recherche/banques/CRORA); no sequence data is available.

Differences in genome organization of rhabdoviruses correlate with taxonomy. The simplest organization is found in lyssaviruses with the classical gene order N-P-M-G-L. Other genera may include additional genes (Tordo et al., 2005). C proteins have been identified in members of the vesiculovirus genus that infect vertebrates (Barik, 1992; Kretzschmar et al., 1996; Marriott, 2005; Peluso et al., 1996; Springfeld et al., 2005). C ORFs were also identified in TUPV (Springfeld et al., 2005), in some novirhabdoviruses (Nishizawa et al., 1997; Schutze et al., 1999) and the unclassified *Siniperca chuatsi* rhabdovirus (SCRV)(Tao et al., 2008). However, in contrast to MOUV, TUPV and novirhabdoviruses possess additional ORFs between their M and G (SH, (Springfeld et al., 2005)), or G and L genes (NV, (Kurath et al., 1997; Schutze et al., 1999)), respectively. Despite divergence in genome organization, dimarhabdoviruses share biological characteristics; they replicate in both invertebrate (**di**pteran) and vertebrate (**ma**mmal) hosts in transmission cycles maintained through hematophagous arthropods (Bourhy et al., 2005). Sequence analysis reveals features consistent with the identification of MOUV as a dimarhabdovirus. L sequence alignment indicates closest relationship to TUPV and TIBV; N shows conservation of aa motifs found in dimarhabdoviruses (Kuzmin et al., 2006); G contains the twelve cysteines conserved in animal rhabdoviruses (Walker and Kongsuwan, 1999); and the 3'-leader sequence conserves the characteristic first three and tenth nt present in rhabdoviruses that infect mammals. Furthermore, MOUV was isolated from *Culex decens* mosquitoes, a species that is primarily ornithophilic but also feeds on bats (Boreham and Snow, 1973). Although we have not been able to replicate MOUV in mammalian cell lines this may only reflect limitations in our repertoire.

Arthropod transmitted diseases remain a major threat to human health worldwide. Chandipura virus, isolated in the late 1960s and transmitted to humans by sandflies, has become a recognized public health threat since the Indian Chandipura encephalitis outbreak in 2003 (Bhatt and Rodrigues, 1967; Rao et al., 2004). Characterizing the wealth of arthropod-borne

agents remains of crucial importance to surveillance efforts and the prediction of disease emergence.

Supplementary Material

Refer to Web version on PubMed Central for supplementary material.

Abbreviations

BHK	baby hamster kidney
FLAV	Flanders virus
G	glycoprotein
IHNV	Infectious hematopoietic necrosis virus
M	matrixs
L	polymerase
MOUV	Moussa virus
N	nucleoprotein
P	phosphoprotein
PCF	primary chicken embryo fibroblasts
PSEK	porcine stable equine kidney
RACE	rapid amplification of cDNA ends
TUPV	Tupaia virus
UHTS	unbiased high throughput sequencing
WONV	Wongabel virus
VSIV	Vesicular stomatitis Indiana virus
VSV	Vesicular stomatitis virus
TIBV	Tibrogargan virus

Acknowledgments

We thank the Ivorian authorities for their long-term support, the Ministry of Environment and Forest, as well as the Ministry of Research, the directorship of the Taï National Park and the Swiss Research Center in Abidjan. The authors are also grateful to the Taï chimpanzee project and Christophe Boesch for logistic support, Stephen Rich for mosquito traps, Germain Gagné for help during field work, Georg Pauli for helpful comments on virus culturing and analyses, Omar Jabado for help with phylogenetic analyses, Craig Street, Raul Rabadan, and Alexander Solovyov for bioinformatic analyses, and Jennifer Decuir for excellent experimental assistance. This work was supported by the Robert Koch-Institute, the Max-Planck-Society, Google.org and National Institutes of Health awards AI051292 and AI57158 (Northeast Biodefense Center - Lipkin).

References

Aitken TH, Kowalski RW, Beaty BJ, Buckley SM, Wright JD, Shope RE, Miller BR. Arthropod studies with rabies-related Mokola virus. Am J Trop Med Hyg 1984;33(5):945–952. [PubMed: 6385743]

Albertini AA, Wernimont AK, Muziol T, Ravelli RB, Clapier CR, Schoehn G, Weissenhorn W, Ruigrok RW. Crystal structure of the rabies virus nucleoprotein-RNA complex. Science 2006;313(5785):360–363. [PubMed: 16778023]

Altschul SF, Gish W, Miller W, Myers EW, Lipman DJ. Basic local alignment search tool. J Mol Biol 1990;215(3):403–410. [PubMed: 2231712]

Barik S. The phosphoprotein (P) gene of the rhabdovirus Piry: its cloning, sequencing, and expression in Escherichia coli. Nucleic Acids Res 1992;20(21):5843. [PubMed: 1454546]

Barik S, Banerjee AK. Phosphorylation by cellular casein kinase II is essential for transcriptional activity of vesicular stomatitis virus phosphoprotein P. Proc Natl Acad Sci U S A 1992;89(14):6570–6574. [PubMed: 1321444]

Bhatt PN, Rodrigues FM. Chandipura: a new Arbovirus isolated in India from patients with febrile illness. Indian J Med Res 1967;55(12):1295–1305. [PubMed: 4970067]

Biel SS, Gelderblom HR. Diagnostic electron microscopy is still a timely and rewarding method. J Clin Virol 1999;13(1–2):105–119. [PubMed: 10405897]

Boreham PF, Snow WF. Letter: Further information on the food sources of Culex (Culex) decens Theo. (Dipt., Culicidae). Trans R Soc Trop Med Hyg 1973;67(5):724–725. [PubMed: 4798389]

Bourhy H, Cowley JA, Larrous F, Holmes EC, Walker PJ. Phylogenetic relationships among rhabdoviruses inferred using the L polymerase gene. J Gen Virol 2005;86(Pt 10):2849–2858. [PubMed: 16186241]

Bujnicki JM, Rychlewski L. In silico identification, structure prediction and phylogenetic analysis of the 2'-O-ribose (cap 1) methyltransferase domain in the large structural protein of ssRNA negative-strand viruses. Protein Eng 2002;15(2):101–108. [PubMed: 11917146]

Chattopadhyay D, Banerjee AK. Phosphorylation within a specific domain of the phosphoprotein of vesicular stomatitis virus regulates transcription in vitro. Cell 1987;49(3):407–414. [PubMed: 3032453]

Chen BJ, Lamb RA. Mechanisms for enveloped virus budding: can some viruses do without an ESCRT? Virology 2008;372(2):221–232. [PubMed: 18063004]

Coll JM. The glycoprotein G of rhabdoviruses. Arch Virol 1995;140(5):827–851. [PubMed: 7605197]

Cox-Foster DL, Conlan S, Holmes EC, Palacios G, Evans JD, Moran NA, Quan PL, Briese T, Hornig M, Geiser DM, Martinson V, vanEngelsdorp D, Kalkstein AL, Drysdale A, Hui J, Zhai J, Cui L, Hutchison SK, Simons JF, Egholm M, Pettis JS, Lipkin WI. A metagenomic survey of microbes in honey bee colony collapse disorder. Science 2007;318(5848):283–287. [PubMed: 17823314]

Demirov DG, Freed EO. Retrovirus budding. Virus Res 2004;106(2):87–102. [PubMed: 15567490]

Desforges M, Charron J, Berard S, Beausoleil S, Stojdl DF, Despars G, Laverdiere B, Bell JC, Talbot PJ, Stanners CP, Poliquin L. Different host-cell shutoff strategies related to the matrix protein lead to persistence of vesicular stomatitis virus mutants on fibroblast cells. Virus Res 2001;76(1):87–102. [PubMed: 11376849]

Dhanda V, Rodrigues FM, Ghosh SN. Isolation of Chandipura virus from sandflies in Aurangabad. Indian J Med Res 1970;58(2):179–180. [PubMed: 5528233]

Green TJ, Zhang X, Wertz GW, Luo M. Structure of the vesicular stomatitis virus nucleoprotein-RNA complex. Science 2006;313(5785):357–360. [PubMed: 16778022]

Harty RN, Paragas J, Sudol M, Palese P. A proline-rich motif within the matrix protein of vesicular stomatitis virus and rabies virus interacts with WW domains of cellular proteins: implications for viral budding. J Virol 1999;73(4):2921–2929. [PubMed: 10074141]

Hayat M, Axon AT, O'Mahony S. Diagnostic yield and effect on clinical outcomes of push enteroscopy in suspected small-bowel bleeding. Endoscopy 2000;32(5):369–372. [PubMed: 10817173]

Igarashi A. Isolation of a Singh's Aedes albopictus cell clone sensitive to Dengue and Chikungunya viruses. J Gen Virol 1978;40(3):531–544. [PubMed: 690610]

Irie T, Licata JM, McGettigan JP, Schnell MJ, Harty RN. Budding of PPxY-containing rhabdoviruses is not dependent on host proteins TGS101 and VPS4A. J Virol 2004;78(6):2657–2665. [PubMed: 14990685]

Junglen S, Kopp A, Kurth A, Pauli G, Ellerbrok H, Leendertz FH. A new flavivirus and a new vector: characterization of a novel flavivirus isolated from uranotaenia mosquitoes from a tropical rain forest. J Virol 2009;83(9):4462–4468. [PubMed: 19224998]

Kaptur PE, McCreedy BJ Jr. Lyles DS. Sites of in vivo phosphorylation of vesicular stomatitis virus matrix protein. J Virol 1992;66(9):5384–5392. [PubMed: 1323702]

Kopecky SA, Willingham MC, Lyles DS. Matrix protein and another viral component contribute to induction of apoptosis in cells infected with vesicular stomatitis virus. J Virol 2001;75(24):12169–12181. [PubMed: 11711608]

Kouznetzoff A, Buckle M, Tordo N. Identification of a region of the rabies virus N protein involved in direct binding to the viral RNA. J Gen Virol 1998;79(Pt 5):1005–1013. [PubMed: 9603315]

Kretzschmar E, Peluso R, Schnell MJ, Whitt MA, Rose JK. Normal replication of vesicular stomatitis virus without C proteins. Virology 1996;216(2):309–316. [PubMed: 8607260]

Kurath G, Higman KH, Bjorklund HV. Distribution and variation of NV genes in fish rhabdoviruses. J Gen Virol 1997;78(Pt 1):113–117. [PubMed: 9010293]

Kuzmin IV, Hughes GJ, Rupprecht CE. Phylogenetic relationships of seven previously unclassified viruses within the family Rhabdoviridae using partial nucleoprotein gene sequences. J Gen Virol 2006;87(Pt 8):2323–2331. [PubMed: 16847128]

Li J, Rahmeh A, Morelli M, Whelan SP. A conserved motif in region v of the large polymerase proteins of nonsegmented negative-sense RNA viruses that is essential for mRNA capping. J Virol 2008;82 (2):775–784. [PubMed: 18003731]

Li J, Wang JT, Whelan SP. A unique strategy for mRNA cap methylation used by vesicular stomatitis virus. Proc Natl Acad Sci U S A 2006;103(22):8493–8498. [PubMed: 16709677]

Luo M, Green TJ, Zhang X, Tsao J, Qiu S. Conserved characteristics of the rhabdovirus nucleoprotein. Virus Res 2007;129(2):246–251. [PubMed: 17764775]

Lyles, DS.; Rupprecht, CE. Rhabdoviridae. In: Knipe, DM.; Howley, PM., editors. Fields Virology. Vol. 1. Philadelphia, Pa: Lippincott Williams & Wilkins; 2007. p. 1394-1408.

Margulies M, Egholm M, Altman WE, Attiya S, Bader JS, Bemben LA, Berka J, Braverman MS, Chen YJ, Chen Z, Dewell SB, Du L, Fierro JM, Gomes XV, Godwin BC, He W, Helgesen S, Ho CH, Irzyk GP, Jando SC, Alenquer ML, Jarvie TP, Jirage KB, Kim JB, Knight JR, Lanza JR, Leamon JH, Lefkowitz SM, Lei M, Li J, Lohman KL, Lu H, Makhijani VB, McDade KE, McKenna MP, Myers EW, Nickerson E, Nobile JR, Plant R, Puc BP, Ronan MT, Roth GT, Sarkis GJ, Simons JF, Simpson JW, Srinivasan M, Tartaro KR, Tomasz A, Vogt KA, Volkmer GA, Wang SH, Wang Y, Weiner MP, Yu P, Begley RF, Rothberg JM. Genome sequencing in microfabricated high-density picolitre reactors. Nature 2005;437(7057):376–380. [PubMed: 16056220]

Marriott AC. Complete genome sequences of Chandipura and Isfahan vesiculoviruses. Arch Virol 2005;150(4):671–680. [PubMed: 15614433]

Nault LR. Arthropod transmission of plant viruses: a new synthesis. Ann. Rev. Entomol.Soc. Am 1997; (90):521–541.

Nishizawa T, Kurath G, Winton JR. Sequence analysis and expression of the M1 and M2 matrix protein genes of hirame rhabdovirus (HIRRV). Diseases of aquatic organisms 1997;31:9–17.

Palacios G, Druce J, Du L, Tran T, Birch C, Briese T, Conlan S, Quan PL, Hui J, Marshall J, Simons JF, Egholm M, Paddock CD, Shieh WJ, Goldsmith CS, Zaki SR, Catton M, Lipkin WI. A new arenavirus in a cluster of fatal transplant-associated diseases. N Engl J Med 2008;358(10):991–998. [PubMed: 18256387]

Palacios G, Quan PL, Jabado OJ, Conlan S, Hirschberg DL, Liu Y, Zhai J, Renwick N, Hui J, Hegyi H, Grolla A, Strong JE, Towner JS, Geisbert TW, Jahrling PB, Buchen-Osmond C, Ellerbrok H, Sanchez-Seco MP, Lussier Y, Formenty P, Nichol MS, Feldmann H, Briese T, Lipkin WI. Panmicrobial oligonucleotide array for diagnosis of infectious diseases. Emerg Infect Dis 2007;13 (1):73–81. [PubMed: 17370518]

Peluso RW, Richardson JC, Talon J, Lock M. Identification of a set of proteins (C' and C) encoded by the bicistronic P gene of the Indiana serotype of vesicular stomatitis virus and analysis of their effect on transcription by the viral RNA polymerase. Virology 1996;218(2):335–342. [PubMed: 8610460]

Poch O, Blumberg BM, Bougueleret L, Tordo N. Sequence comparison of five polymerases (L proteins) of unsegmented negative-strand RNA viruses: theoretical assignment of functional domains. J Gen Virol 1990;71(Pt 5):1153–1162. [PubMed: 2161049]

Poch O, Sauvaget I, Delarue M, Tordo N. Identification of four conserved motifs among the RNA-dependent polymerase encoding elements. Embo J 1989;8(12):3867–3874. [PubMed: 2555175]

Rao BL, Basu A, Wairagkar NS, Gore MM, Arankalle VA, Thakare JP, Jadi RS, Rao KA, Mishra AC. A large outbreak of acute encephalitis with high fatality rate in children in Andhra Pradesh, India, in 2003, associated with Chandipura virus. Lancet 2004;364(9437):869–874. [PubMed: 15351194]

Rice P, Longden I, Bleasby A. EMBOSS: the European Molecular Biology Open Software Suite. Trends Genet 2000;16(6):276–277. [PubMed: 10827456]

Schmitt AP, Lamb RA. Escaping from the cell: assembly and budding of negative-strand RNA viruses. Curr Top Microbiol Immunol 2004;283:145–196. [PubMed: 15298170]

Schutze H, Mundt E, Mettenleiter TC. Complete genomic sequence of viral hemorrhagic septicemia virus, a fish rhabdovirus. Virus Genes 1999;19(1):59–65. [PubMed: 10499451]

Shope RE. Rabies-related viruses. Yale J Biol Med 1982;55(3–4):271–275. [PubMed: 6758373]

Springfeld C, Darai G, Cattaneo R. Characterization of the Tupaia rhabdovirus genome reveals a long open reading frame overlapping with P and a novel gene encoding a small hydrophobic protein. J Virol 2005;79(11):6781–6790. [PubMed: 15890917]

Stang A, Korn K, Wildner O, Uberla K. Characterization of virus isolates by particle-associated nucleic acid PCR. J Clin Microbiol 2005;43(2):716–720. [PubMed: 15695669]

Tao JJ, Zhou GZ, Gui JF, Zhang QY. Genomic sequence of mandarin fish rhabdovirus with an unusual small non-transcriptional ORF. Virus Res 2008;132(1–2):86–96. [PubMed: 18068257]

Tesh RB, Chaniotis BN, Johnson KM. Vesicular stomatitis virus (Indiana serotype): transovarial transmission by phlebotomine sandlies. Science 1972;175(29):1477–1479. [PubMed: 4335268]

Thomas D, Newcomb WW, Brown JC, Wall JS, Hainfeld JF, Trus BL, Steven AC. Mass and molecular composition of vesicular stomatitis virus: a scanning transmission electron microscopy analysis. J Virol 1985;54(2):598–607. [PubMed: 2985822]

Thompson JD, Gibson TJ, Higgins DG. Multiple sequence alignment using ClustalW and ClustalX. Chapter 2, Unit 2 3. Curr Protoc Bioinformatics. 2002

Tordo N, Benmansour A, Calisher C, Dietzgen RG, Fang RX, Jackson AO, Kurath G, Nadin-Davis S, Tesh RB, Walker PJ. Virus Taxonomy. Eighth Report of the International Committee on Taxonomy of Viruses 2005:623–644.

Tuffereau C, Fischer S, Flamand A. Phosphorylation of the N and M1 proteins of rabies virus. J Gen Virol 1985;66(Pt 10):2285–2289. [PubMed: 2995564]

Walker PJ, Kongsuwan K. Deduced structural model for animal rhabdovirus glycoproteins. J Gen Virol 1999;80(Pt 5):1211–1220. [PubMed: 10355768]

Whelan SP, Barr JN, Wertz GW. Transcription and replication of nonsegmented negative-strand RNA viruses. Curr Top Microbiol Immunol 2004;283:61–119. [PubMed: 15298168]

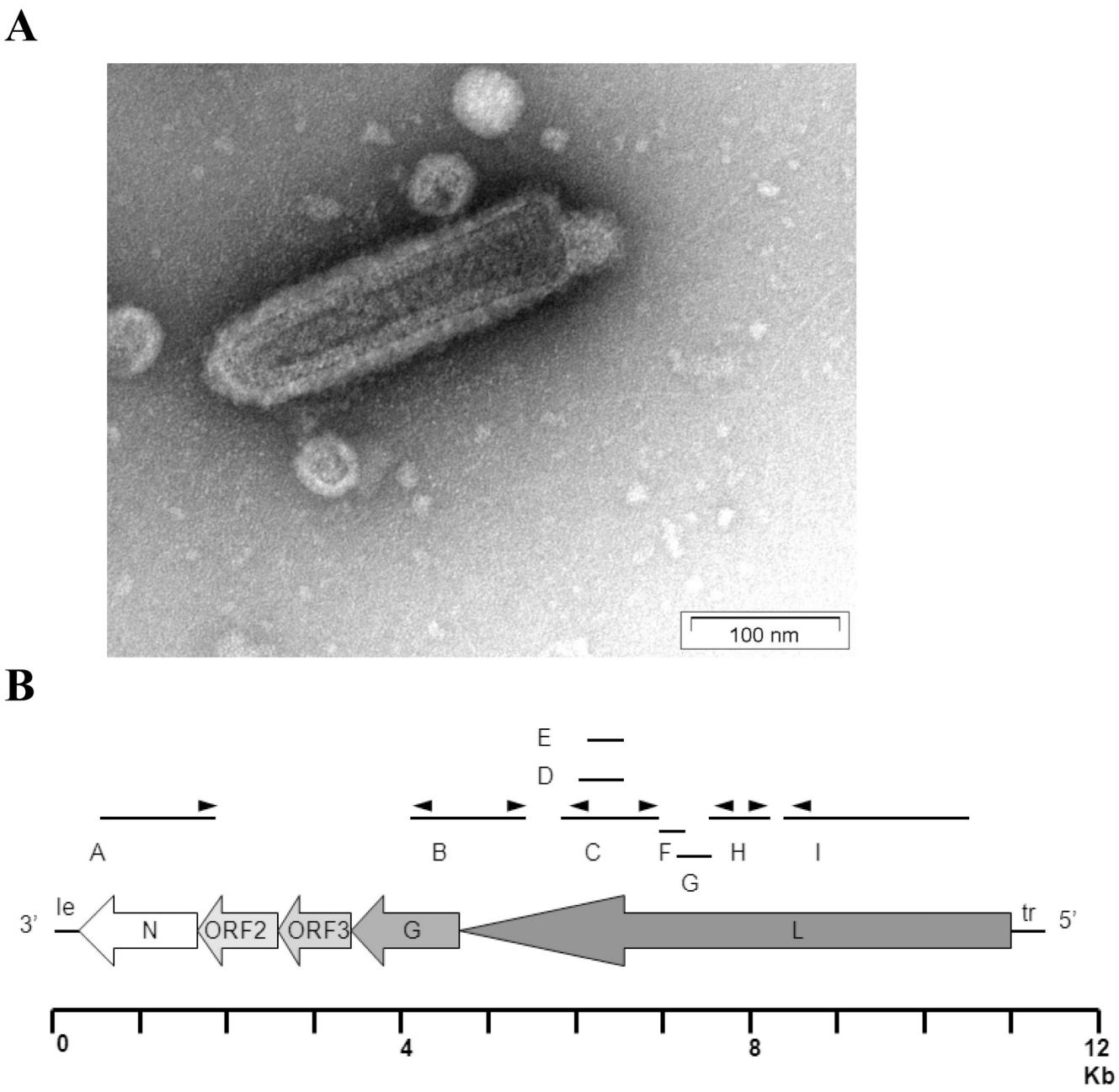

Fig. 1.

Morphology and schematic of genome organization of MOUV. (**A**) MOUV C23 in negative contrast electron microscopy. (**B**) Arrows represent the five open reading frames (ORF) of the 11,526 nt single strand, negative sense genome. Bars above the schematic indicate the 9 contigs (A to I, Table 1) generated through UHTS. Arrowheads indicate primer locations (Table S1). le: leader; tr: trailer. N: nucleoprotein; ORF2: putative phosphoprotein; ORF3: putative matrix; G: glycoprotein; L: polymerase.

A

Gene junction	Gene end	Intergenic	Gene start
Leader-N			UUGUUUGAAGUAUUCAGUCACUUUUAC
N-ORF2	AUU(X)$_{38}$GAACUUUUUUU	GUG	UUGUUUGGAGUAUUCUCGCUUGUGUAAUAC
ORF2-ORF3	AUU(X)$_{22}$GAACUUUUUUU	CUA	UUGUUUGGAUUAUGCAAUGUUCUAC
ORF3-G	AUU(X)$_{34}$GAACUUUUUUU	AG	UUGUGUGGAGUAACCUAAGAUG(X)$_{38}$UAC
G-L	ACU(X)$_{79}$GAACUUUUUUU	CA	UUGUUUGCACUAAAUAGAUUGCAGAUAUUAUUUUAC
L-Trailer	AUUCGUCAUGAACUUUUUUU		
	**********		**** ** * **
MOUV	GAACUUUUUUU	2 - 3 nt	UUGUKUGVABUA
TUPV	GWWCUUUUUUU	G(G)	UUGMCCNKNAG
VSIV	AUACUUUUUUU	SU	UUGUCNNUAGR
BEFV	GUACUUUUUUU	21 - 47 nt	UUSUCCNKNNN
RABV	RNACUUUUUUU	2 - 423 nt	UUGURRNGANN
IHNV	URUCUUUUUUU	R	CCGUGNNNNCA
NCMV	AUUCUUUUU	GA	CUCU

B

```
Leader   3′-UGCUAUGUUUCUUUGCGGUUAAUAUAGGUGGUGUAAAUCCCCACUUGGGAGAGUUGUUUGAAGUAUUCAGUCACUUUUAC
            ||||||  |||   |  ||||||||   ||||
Trailer  5′-ACGAUAAAAAAUACCGCCAAUAGAAUCGCUAAUGAACAAAGGACGAUCUUCUCUGGUUUUUUUCAAGUACUGCUUA
```

C

MOUV	3′-**UGC**UAUGUU**U**CUUUGCGGUUAAUAUAGGUGGUGUAAAUCCCCACUUGGGAGAGUUGUUUGAAGUAUUCAGUCACUUUUAC-5′
TUPV	3′-**UGC**UUCUGU**U**GUUUUGUUAGUUUCCCCUAAUUAACCAAGCCUCAACAGAUGAGAUUCGGAAUUGCCCUUGA-5′
VSIV	3′-**UGC**UUCUGU**U**UGUUUGGUAAUAAUAGUAAUUUUCCGAGUCCUCUUUGAAAUUGUCAUUAG-5′
SVCV	3′-**UGC**AUCAGU**U**UUACAGGCAACUACUGUAAUGUACCAAAUAAACAGAAGUCUUUUUACCAUUGUCUGUAG-5′
BEFV	3′-**UGC**UCUUUU**U**UGUUUUUUUGAUAACUAUAACUAUGGGUUAAUCACAAAGUUGUCCAGAG-5′
RABV	3′-**UGC**GAAUUG**U**UGGUCUAGUUUCUUUUUUGUCUGUCGCAGUUACCGUCUCGUUUUUACAUUGUGGAGAU-5′
MOKV	3′-**UGC**GAAUUG**U**UGGUCUAGUUUCUUCUGUGUCUAUCAUAGUCACUGGAUUUGUUUUACAUUGUGAGGAU-5′
COCV	3′-**UGC**UUCUGU**U**UGUUUGGUAAUUAUAUUAAUUUUCCGAGUC-5′

Fig. 2.

Identification of MOUV sequence motifs and comparison with other rhabdoviruses. (**A**) Sequences at the gene junctions. Gene end, intergenic and gene start regions of the five MOUV genes are shown (upper panel). Sequence at the gene junctions of MOUV was compared to that of other rhabdoviruses (lower panel). Asterisk indicates bases identity. The complement of start and stop codons is underlined. (**B**) Complementarity of the leader and the trailer of

MOUV. The complement of start and stop codons is underlined. (**C**) Comparison of the MOUV leader with that of other rhabdoviruses. Conserved nucleotides are indicated in bold.

A

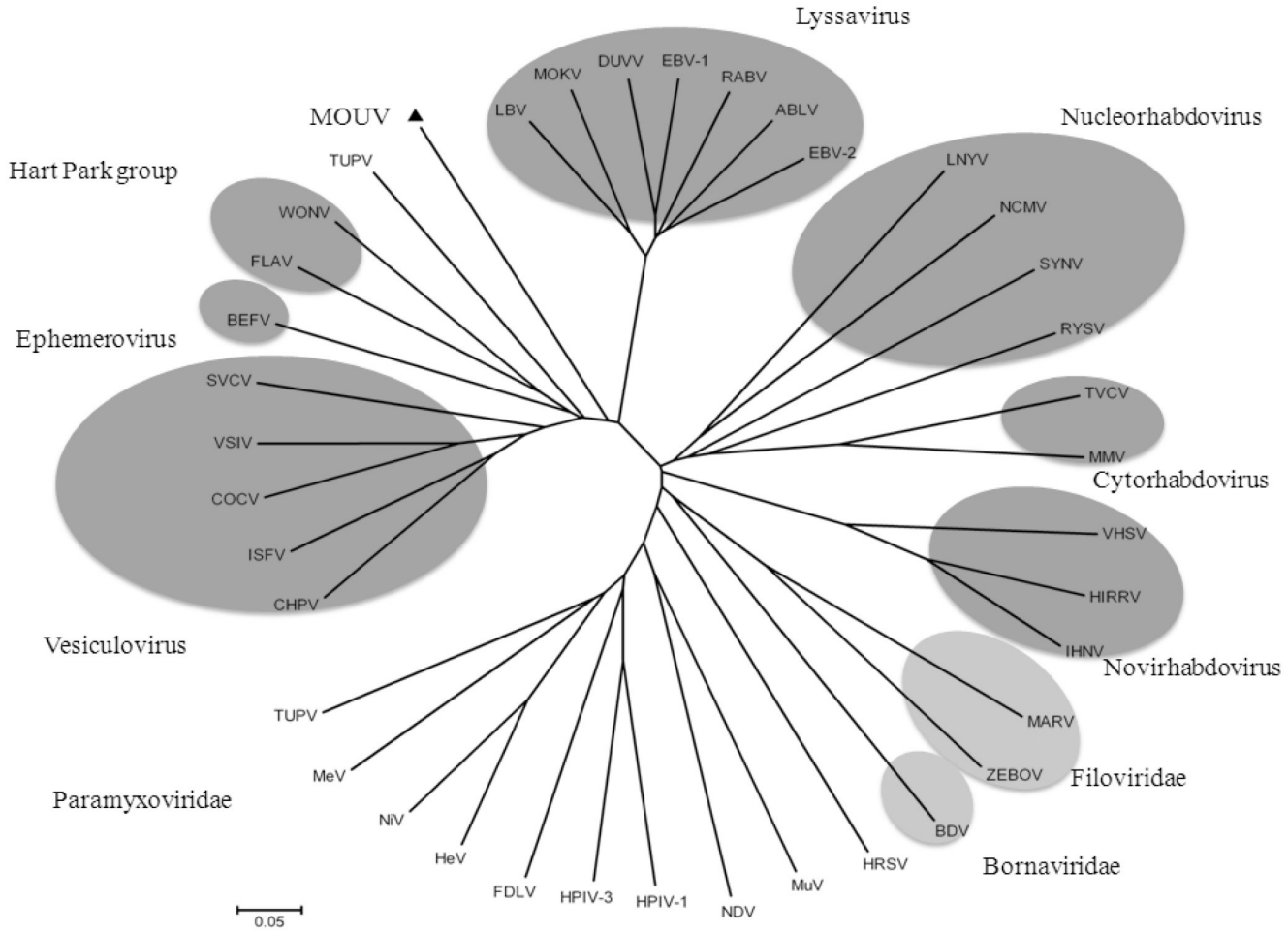

B

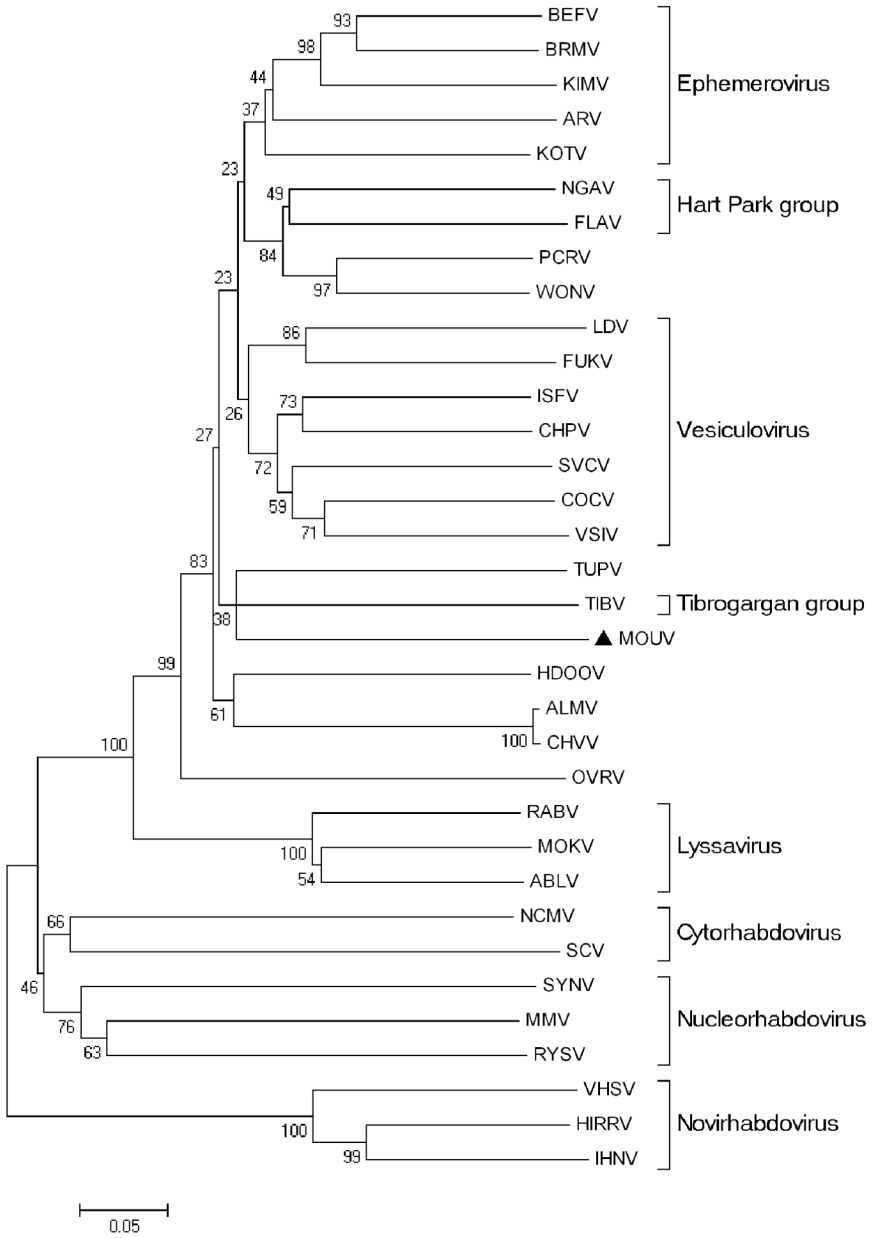

Fig. 3.

Phylogenetic analysis of full-length (**A**) and partial (**B**) L protein sequences. (A) deduced L amino acid sequence of MOUV was analyzed in comparison to available full-length L sequences of other rhabdoviruses (dark grey) and other selected members of the order *Mononegavirales* (light grey). (B) Partial L sequence (aa 560–700) including the additional rhabdovirus sequences available for this region were analyzed. For virus abbreviations see Table S2.

Table 1

Contigs generated by UHTS that show homology to rhabdoviruses by blastn/x

Contig	Reads*	Mean read length (bp)	Contig length (bp)	Gene region	Genome position
A	99	232	1,579	N-ORF2	351 – 1,929
B	192	238	1,578	G-L	3,522 – 5,099
C**	124	232	1,427	L	5,629 – 7,055
D	2	274	220	L	5,859 – 6,078
E	3	173	164	L	5,916 – 6,079
F	1	na	116	L	7,036 – 7,151
G	2	140	162	L	7,122 – 7,283
H	257	215	764	L	7,301 – 8,064
I	178	226	2,672	L	8,125 – 10,796

* Number of sequence reads comprising the contig; na: not applicable

** Identified by blastn alignment; all other contigs identified by blastx alignment

Table 2

Contigs generated by UHTS that map to MOUV genome sequence

	A *		B	
Gene	**No. of reads**	**Mean read length (bp)**	**No. of reads**	**Mean read length (bp)**
N	99	232	119	221
ORF2 (P)	0	na	31	223
ORF3 (M)	0	na	352	245
G	192	238	226	235
L	567	210	852	210
	858	226	1 572	222

* Column A lists the initial analysis, while column B indicates additional reads identified by comparison to the final MOUV genome sequence. na: not applicable.

Table 3

Sequence identity (I) and similarity (S) between MOUV (isolate D24) and other rhabdoviruses

Virus	Genus	N		ORF2[a]		ORF3[b]		G		L	
		I	S	I	S	I	S	I	S	I	S
SYNV	Nucleorhabdovirus	16.1	26.1	12	21	15.4	22.7	13.8	21.3	17.4	27.7
LNYV	Cytorhabdovirus	15.3	25	14	20.7	16.5	22.2	12.7	19.8	18	29.5
IHNV	Novirhabdovirus	15.7	23.3	15.3	24.1	13.4	21.7	**23.2**	**36**	18.5	31.1
BEFV	Ephemerovirus	20.3	36.2	16.2	23.3	15.3	23.6	14.3	25.6	29.7	45.8
ABLV	Lyssavirus	22.1	36.9	16.2	26.8	15.3	22.6	22	33.1	29.5	46.3
EBV-1	Lyssavirus	20.6	34.7	15.6	27.9	16.8	28	19.5	30.4	29.4	46
EBV-2	Lyssavirus	17.6	31.8	15.8	24.6	13.8	19.2	21.7	36.1	29.2	46
MOKV	Lyssavirus	20.6	36	19.2	28.8	15.1	25.6	20.1	33.4	28.6	44.9
RABV	Lyssavirus	21	35.4	14	23.1	10.4	17.8	20.8	32.9	29.5	47
VSIV	Vesiculovirus	**23.5** *	40.2	17.8	29	14.4	24.3	22.9	35.5	**32.6**	**48.3**
COCV	Vesiculovirus	21.8	**42.2**	17.8	27.3	17.7	32.3	20.9	35.6	31.4	46.4
CHPV	Vesiculovirus	22.5	38.1	17.4	27.7	16.6	29.6	19.9	32.7	31.1	47.4
ISFV	Vesiculovirus	17.9	32.9	19.3	29.7	16.8	26.4	20.4	31.8	30	45.7
TUPV	Tentative Vesiculovirus	23	38	12.9	18.8	14.3	25.4	20.7	33	31.4	47.3
FLAV	Hart Park Group	20.4	34.3	19.6	28.8	19	30.3	18.1	32.1	30.5	46.6
WONV	na	22.6	36.4	**20.9**	**30.1**	**20.7**	**35**	20.3	33.3	30	46.8

* Highest values for each gene are shown in bold; na; not applicable

[a] ORF2: genomic position of P

[b] ORF3: genomic position of M

Table 4

Comparison of MOUV L polymerase motifs with those other rhabdoviruses

	Motif A	Motif B	Motif C	Motif D
MOUV	ANSL**D**YD**K**WNNN**QR** *	VCWN**G**QQ**GG**F**EGL**R**Q**KG**W**SVVNYLIL	IL**AQGDN**QII	YRGKIIALES**K**RW
RABV	AFHL**D**YE**K**WNNH**QR**	TCWN**G**QD**GGLEGL**R**Q**KG**W**SLVSLLMI	VL**AQGDN**QVL	FRGNILVPES**K**RW
VSIV	ANHI**D**YE**K**WNNH**QR**	VCWQ**G**QE**GGLEGL**R**Q**KG**W**TILNLLVI	VL**AQGDN**QVI	FRGVIRGLET**K**RW
BEFV	ANNI**D**YE**K**WNNY**QR**	VCWE**G**QK**GGLEGL**R**Q**KG**W**SILNYLMI	IL**AQGDN**QTI	IEGTIKGLPT**K**RW
CHPV	ANHI**D**YE**K**WNNH**QR**	VCWN**G**QA**GGLEGL**R**Q**GG**W**SILNYIQR	VL**AQGDN**QVI	FRGVIRGLET**K**RW
VHSV	SKSL**D**IN**K**FCTS**QR**	GAFS**G**LM**GGIEGL**C**Q**YV**W**TICDLLRV	VM**AQGDN**VII	HCPQHDTLAV**K**KA
TUPV	SNHL**D**YS**K**WNNH**QR**	VCWN**G**QA**GGLEGL**R**Q**KG**W**SIVNLLLI	IL**AQGDN**QVM	FRGNITIPES**K**KW
WONV	ANHI**D**YE**K**WNNH**QR**	VCWN**G**QK**GGLEGL**R**Q**KG**W**SVLNYIER	VL**AQGDN**QTI	FRGVIRGLHL**K**RW

* Strictly conserved residues are shown in bold.

Table 5

Pools of female mosquitoes infected with MOUV

Pool	Mosquito species	Trap location	Trap height	Pool size
A8	*Culex* spp	camp site	1 m	17
B24	*Culex* spp	primary forest	8 m	3
B66	not determined	primary forest	32 m	9
C15	not determined	secondary forest	8 m	6
C21	*Culex decens*	secondary forest	8 m	19
C23	*Culex decens*	secondary forest	16 m	6
D24	*Culex* spp	coffee plantations	1 m	23